

MPPT Controller for PV Array under Partially Shaded Condition

Abd Essalam BADOUD¹

¹Automatic laboratory of Setif, Electrical engineering department, University of Setif 1
City of Maabouda, Algeria

*Corresponding author; Email: badoudabde@univ-setif.dz

Article Info

Article history:

Received 28 April, 2019

Revised 19 May, 2019

Accepted 23 May, 2019

Keywords:

Photovoltaic system

Maximum power point tracking

Shaded condition

Bond graph

Controller

Shading

ABSTRACT

The output power of the Photovoltaic system having multiple arrays is reduced to a great extent when it is partially shaded due to environmental hindrances. Conventional popular MPPT methods are effective under uniform solar irradiance. However, under partially shaded conditions, these MPPTs can fail to track the real MPP because of the multiple local maxima which can be existed on PV characteristic curve under partially shaded condition. This paper reports the development of a maximum power-point tracking method for photovoltaic systems under partially shaded conditions using bond graph. The major advantages of the proposed method are simple computational steps, faster convergence, and its implementation on a low-cost microcontroller. The performance of proposed MPPT is analyzed according to the position of real MPP. Simulation results have been contrasted with real measured data from a commercial PV module of Photowatt PW1650.

I. Introduction

Sustainability and development of new energy resources are one of the important issues globally. It is due to the rise in world oil prices, the protocol that each country is encouraged to increase alternative sources of energy and the demand of ever increasing energy needs [1].

In the recent years, Algeria has approved its determination to contribute to the world efforts to combat the global warming and protect the environment. Throughout this goal, a dynamic green energy has been initiated by launching an ambitious program of development of renewable energy and energy efficiency. This vision is based on a strategy focused on the development of inexhaustible resources, such as solar energy. Photovoltaic (PV) system is one of the potential renewable energy sources which being continuously developed and attracted much attention worldwide.

The reduction of output power in PV modules can be attributed to many factors, but may be the most important are mismatch effects and shadows. Most manufacturers include bypass diodes in their PV modules in order to prevent hot spot formation, in partial shadowing conditions of work. Hot spots appear when a solar cell, normally forming part of a solar cell string of serially connected solar cells, becomes reverse biased and dissipates power in form of heat [2].

The most important component that affects the accuracy of the simulation is the PV cell model. Modeling

of PV cell involves the estimation of the I–V and P–V characteristics curves to emulate the real cell under various environmental conditions. The most popular approach is to utilize the electrical equivalent circuit, which is primarily based on diode. Many models have been proposed by various researchers; the simplest is the basic single-diode model. It comprises of a linear independent current source in parallel to a diode [3; 6]

Once the appropriate model and its computational model have been identified, a complete PV system simulation can be developed. A good PV simulation package should fulfill the following criteria: (1) it should be fast but can accurately predict the I–V and P–V characteristic curves; including special conditions such as partial shading (2) it should be a comprehensive tool to develop and validate the PV system design inclusive of the power converter and MPPT control. Although existing software packages like PSpice, Solar Pro, PV cad, and PV syst are available in the market, they are expensive, unnecessarily complex and rarely support the interfacing of the PV arrays with power converters [7]. Over the years, several researchers have studied the characteristics of PV modules under partial shading condition, [8].

There exist many papers containing the analysis of the behavior of the photovoltaic PV cells under partial shadowing [9;11], taking into account the diode. But there are only a few that actually take into account the importance of the diodes configuration [8]. This article studies the individual behavior of a PV module and a photovoltaic array of PV modules (PV array) connected to an inverter with shadows in both cases. Prior experiments have been conducted investigating the effect of shade on various PV systems, many of which were cited in a comprehensive literature review by Woyte et al. [11] Other recent works include simulations of partially shaded PV cells [12], [13] experimental results of different maximum power point tracking algorithms under shaded conditions [14] and the effect of shade on PV system performance [15], [16].

In view on the importance of this issue, this paper proposes a practical modeling and simulation method, which can predict the I–V and P–V characteristics of large PV arrays. In this paper, a new MPPT method for PV array under partial shading conditions is proposed. The operating principle and structure of proposed method is represented and the operation characteristics of the proposed MPPT are analyzed according to the various positions of real MPP as well as the change in solar irradiance. The simulation and experimental results are presented to verify the performance of proposed method.

II. Bond graph modeling

A bond graph is a labeled and directed graphical representation of a physical system. The basis of bond graph modeling is power/energy flow in a system. As energy or power flow is the underlying principle for bond graph modeling, there is seam less integration across multiple domains. As a consequence, different domains (such as electrical, thermal...) can be represented in a unified way. The power or the energy flow is represented by a half arrow, which is called the power bond or the energy bond [17], [18]. One of the advantages of bond graph method is that models of various systems belonging to different engineering domains can be expressed using a set of only nine elements.

III. System Configuration

One of the main causes of losses in energy generation within photovoltaic systems is the partial shading on photovoltaic. These PV modules are composed of photovoltaic cells (PV cells) serial or parallel connected, with diodes included in different configurations. The curve of a PV cell varies depending on the radiation received and its temperature. Furthermore, the modules have diodes that allow the current flows through an alternative path, when enough cells are shaded or damaged. There are two typical configurations of bypass diodes: overlapped (Fig. 1a) and no-overlapped (Fig. 1b). It should be noted that the analysis in modules with overlapped diodes is a more complex one, because there may be different paths for current flow.

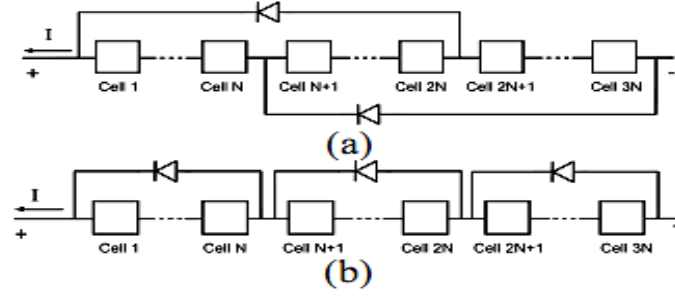


Figure 1. Bypass diodes
(a) overlapped, (b) no-overlapped

IV. Methodology

IV.1. Photovoltaic generator model

The solar cell is basically a p-n junction diode, and its traditional equivalent circuit may express itself similar to what is shown in figure (2).

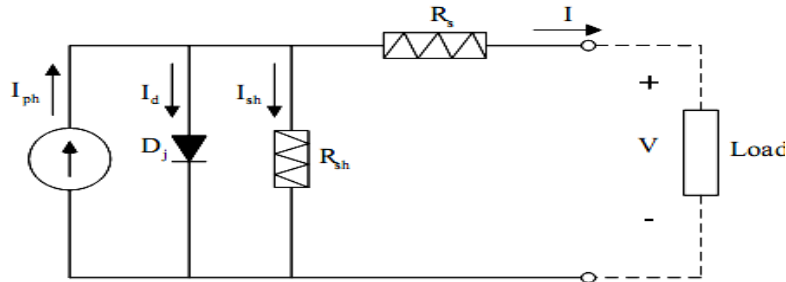


Figure 2. Solar-cell equivalent circuit

According to the physical property of p-n semiconductor, the V-I characteristics of PV module could be expressed as equation (1) [31] - [32].

$$I(1 + R_s / R_{sh}) = -n_p I_{sat} \left[\exp \left\{ \left(\frac{q}{AKT} \right) \left(\frac{V}{n_s} + IR_s \right) \right\} - 1 \right] + n_p I_{ph} - \frac{(V - n_s)}{R_{sh}} \quad (1)$$

In addition, the module reverse saturation current I_{sat} shown in equation (2) is varied with temperature T .

$$I_{sat} = I_{rr} \left(\frac{T}{T_r} \right)^3 \exp \left\{ \left(\frac{qE_{gap}}{kA} \right) \left(\frac{1}{T_r} - \frac{1}{T} \right) \right\} \quad (2)$$

The I_{ph} expressed in equation (3) represents the photocurrent proportionally produced to the level of cell surface temperature and radiation.

$$I_{ph} = \{I_{ss0} + k_i (T - T_r)\} \frac{S_i}{100} \quad (3)$$

For the bond graph representation, the PV generator is then modeled by a flow source $Sf = I_{ph}$ in parallel with two resistors R_{diode} and R_{sh} , the whole followed by a serial resistance R_s . The diode element is labeled R_{diode} , it produces a non-linear current that is essentially exponential in nature:

$$J_{Rd} = J_s \left[\exp \left(\frac{qV}{kT} \right) - 1 \right]. \quad (4)$$

The regular diode is non-linear resistor, as its constitutive equation relates voltage across and current through the diode to each other, an effort flow relationship in bond graph terminology.

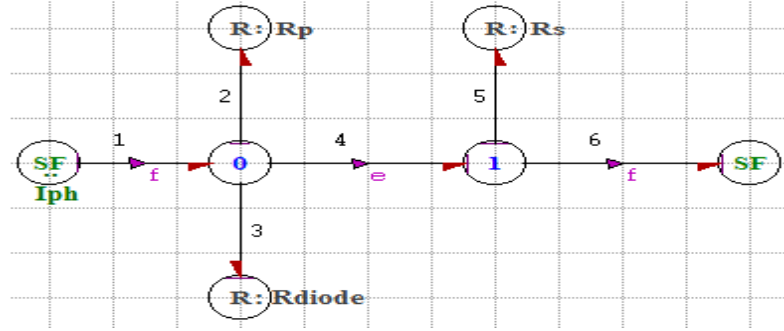


Figure 3. Bond graph model of PV

IV.2. Electrical energy converter modeling

A buck-boost converter provides an output voltage which can be controlled above and below the input voltage level. The output voltage polarity is opposite to that of the input voltage. Figure (4) shows the circuit diagram of a buck-boost converter. This converter either steps up or steps down the input DC voltage fed from the diode rectifier. The converter consists of a DC input voltage source V_i , inductor L , controlled switch K , filter capacitor C and diode D .

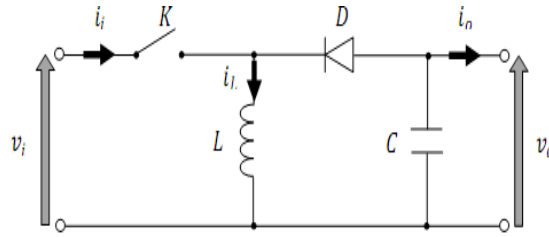


Figure 4. Equivalent circuit of a buck-boost converter

According to the above circuit, we obtain the dynamic equation of the buck-boost converter as follow:

$$\begin{cases} C \frac{\partial v_o}{\partial t} = -d i_o (1-d)(i_L - i_o) \\ L \frac{\partial i_L}{\partial t} = -d v_i + (1-d) v_o \\ i_i = d i_L \end{cases} \quad (5)$$

Where d is the duty ratio of the power switch k ; v_i and v_p are the input and output voltage; i_i , i_o and i_L are the input, output and inductance current. The bond graph model of the buck-boost is thus given by the figure (5).

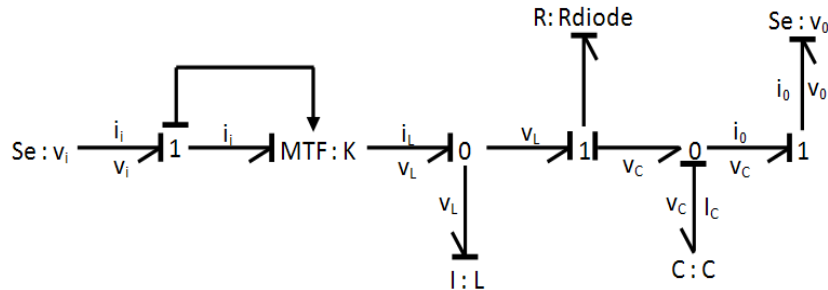


Figure 5. Bond graph model equivalent circuit of buck-boost converter

Reversible current DC/DC converter: to ensure the charge and the discharge of the storage battery, the current must be reversible so that the energy transfer would be in the two directions, from the DC-Bus to the battery and vice versa. For that a Reversible current DC/DC converter is necessary, it's realized by associating a boost chopper and a buck we as shown in figure (6).

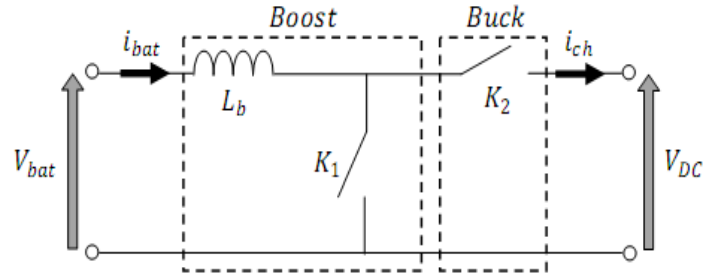


Figure 6. Equivalent circuit of a the reversible current DC/DC converter

The control of the switches k_1 and k_2 is simultaneous with a complementary duty cycles d_b and $1 - d_b$, the reversible current DC/DC converter shown in figure (7) is described the equation (4.2), as:

$$\frac{\partial i_{bat}}{\partial t} = \frac{1}{L} (d_b V_{DC} - V_{bat}) \quad (7)$$

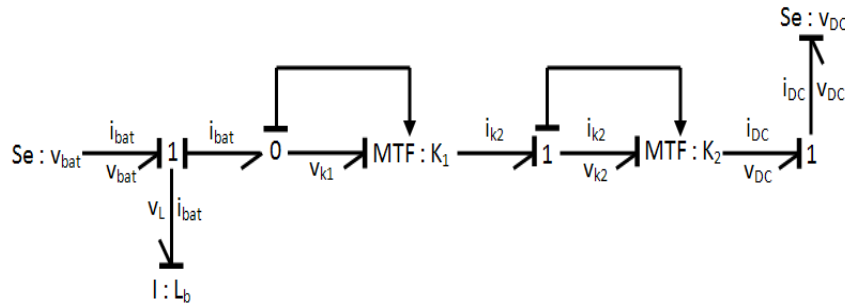


Figure 7. Bond graph model of equivalent circuit of a the reversible current DC/DC converter

IV.3. MPPT Algorithms under partial shading

P&O and the incremental conductance algorithms are the most common. These techniques have the advantage of an easy implementation but they also have drawbacks. In normal conditions the V-P curve has only one maximum, so it is not a problem. However, if the PV array is partially shaded, there are multiple maxima in these curves. In order to relieve this problem, we proposed a new algorithm. the proposed MPPT method uses the simple linear function for tracking under partial shading without any additional circuit. The flowchart of proposed MPPT is represented in figure (8).

Bond graph MPPT can provide a dynamic graphical model to describe non-linear characteristics. For a small-scale PV conversion system, the proposed method is validated by simulation with different operation environments

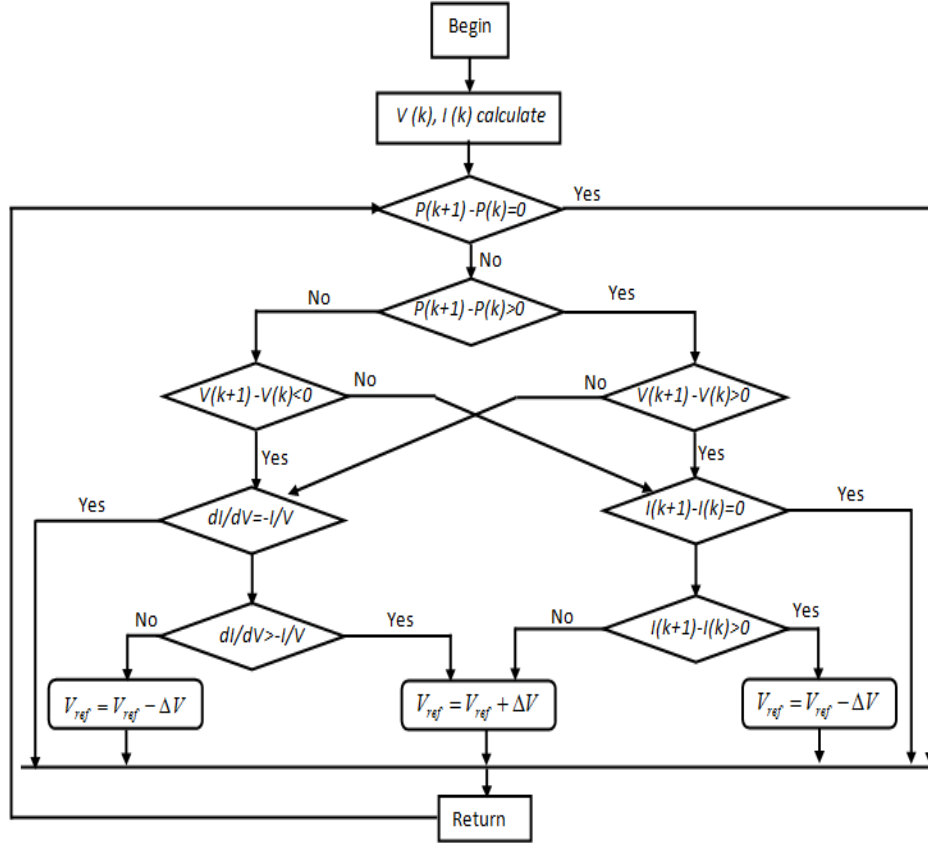


Figure 8. Flowchart of BG-MPPT controller

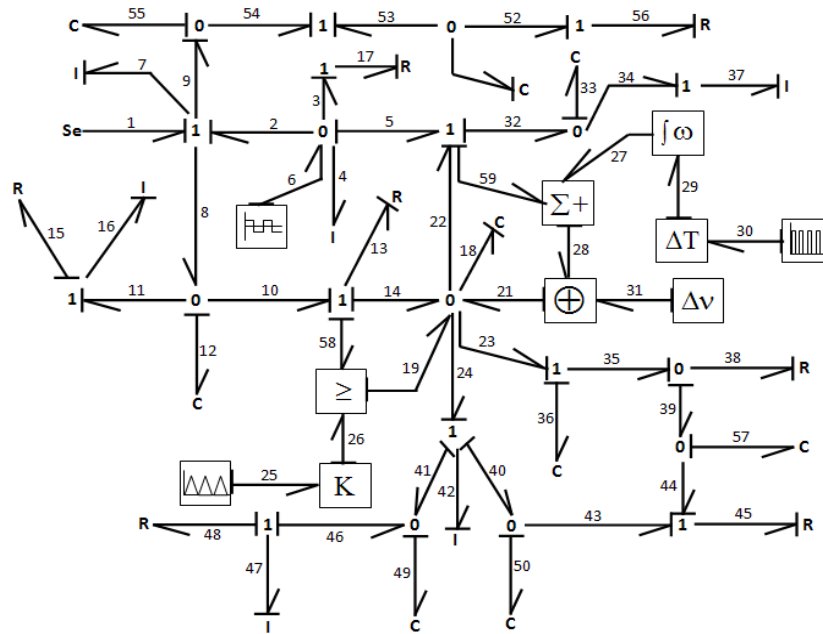


Figure 9. Bond graph controller

In this work, the bond graph control MPPT method has two input variables, namely $\Delta P(k)$ and $\Delta U(k)$, at a sampling instant k . The output variable is $\Delta U(k+1)$, which is voltage's increase of PV array at next sampling instant $k+1$. The variable $\Delta P(k)$ and $\Delta U(k)$ are expressed as follows:

$$\Delta P(k) = P(k) - P(k-1) \quad (8)$$

$$\Delta U(k) = U(k) - U(k-1) \quad (9)$$

Where $P(k)$ and $U(k)$ are the power and voltage of PV array, respectively. So, $\Delta P(k)$ and $\Delta U(k)$ are zero at the maximum power point of a PV array.

In figure (9), e_{25} , SE_1 and e_6 are the converter switching duty ratio, the demanded cell voltage and the actual cell voltage in the j th MPPT cycle, where $j = k, k+1$.

The MPPT controller calculates the new cell voltage set point based on the converter switching duty ratios and the measured cell voltages in the past and at present. The lead compensator (e_{27}) forces the cell voltage to follow the demanded cell voltage signal. In the practical design of the control software, the threshold ε , which is a small positive number close to zero, is used to determine whether the MPP has been reached and e_{26} is used as a positive increment in the demanded cell voltage. The variable δ_j can be defined as:

$$\delta_1 = e_2 + e_4 + e_5 - e_3 \quad (10)$$

$$\delta_2 = e_{31} - e_{28} \quad (11)$$

$$\delta_3 = e_{31} + (e_2 + e_4 + e_5 - e_3) \frac{\delta_2}{\delta_1} \quad (12)$$

When $|\delta_1| > \varepsilon$, the MPPT controller can be simplified as:

$$SE_1(k+1) = SE_1(k) + e_{20}, \delta_3 > \varepsilon_3 \quad (13)$$

$$SE_1(k+1) = SE_1(k), |\delta_3| > \varepsilon_3 \quad (14)$$

$$SE_1(k+1) = SE_1(k) - e_{20}, \delta_3 < -\varepsilon_3 \quad (15)$$

When $|\delta_1| < \varepsilon_1$, the MPPT controller can be simplified as:

$$SE_1(k+1) = SE_1(k) + e_{20}, \delta_2 > \varepsilon_2 \quad (16)$$

$$SE_1(k+1) = SE_1(k), |\delta_2| < \varepsilon_2 \quad (17)$$

$$SE_1(k+1) = SE_1(k) - e_{20}, \delta_2 < -\varepsilon_2 \quad (18)$$

V. Experimental Test

In order to verify some of the simulated curves of the previous section, an experiment was conducted on a PHOTOWATT PW1650 multi-crystalline silicone PV panel using a PVPM 1000C40 curve tracer. The electrical specs of the 165 W panels are described in Table 1.

Table 1. Parameters of the PV module

| Parameters | Value and units |
|--------------------------------|-----------------|
| Maximum power P_{max} | 165W |
| Current peak power I_{mp} | 4.8 A |
| Voltage peak power V_{mp} | 34.4 V |
| Short circuit current I_{sc} | 5.1 A |
| Open circuit voltage V_{oc} | 43.2 V |
| Bypass diodes | 4 |
| Number of cells per module | 72 |

The PHOTOWATT PW1650 photovoltaic panel has the electrical configuration of the cells and bypass diodes. To create a partial shadowing condition, 18 cells belonging to the 2 string were covered with a sheet of cardboard, which makes the shadowing close to 100%, i.e., near zero solar irradiation on the covered area.

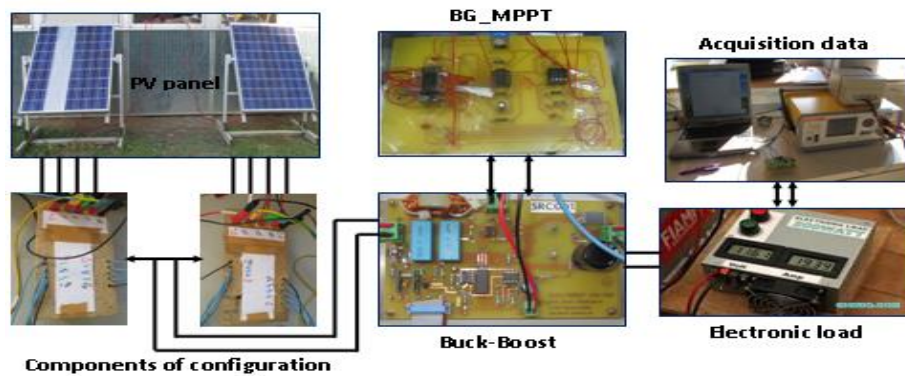


Figure 10. The experimental benchmark

V.1. Limits of inverter

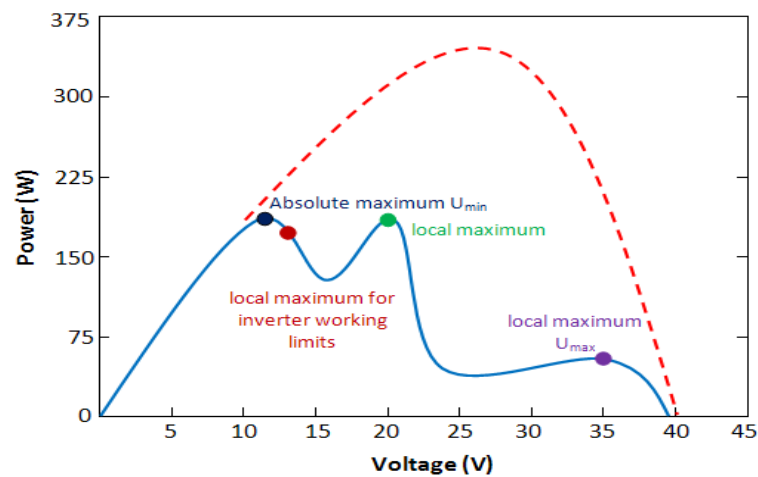


Figure 11. Maximum and local power points of a P-V curve

An inverter that is connected to the PV array can't always achieve the MPP because of his voltage range of work and the tracking MPP algorithm. In figure 11, where the P-V curve is represented, there are four types of points where the inverter could think that there it is the MPP. The inverter can only work in three of them. The absolute maximum is out of its working voltage range.

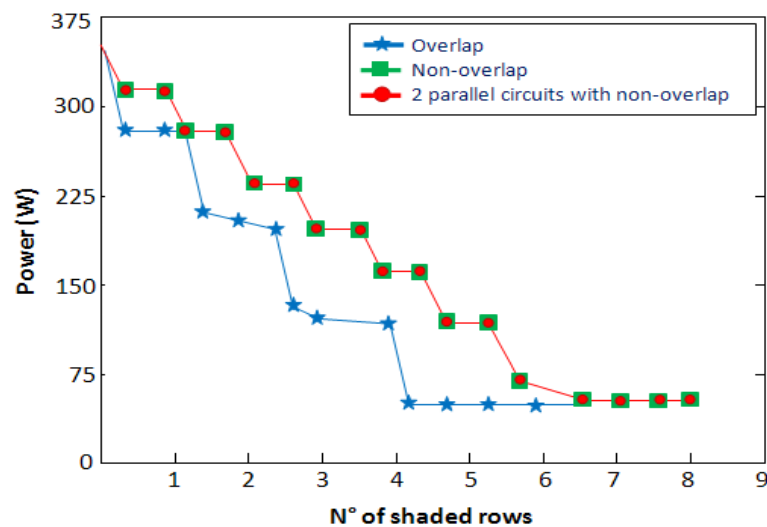


Figure 12. Maximum MPPs of the PV arrays in function of the bottom rows shaded

Figure (12) shows the different types of MPPs against the number of inferior rows shaded in the PV array for the different configurations. On examination, in configuration A, the power losses can reach 40%, while in configuration B and C the losses are 20%. Also, the same power is generated if 12 rows are shaded in configuration A, 20 rows in configuration B and 16 in C. In other words, the PV arrays with bypass diodes (Configuration A) are more susceptible to lose power due to the shadowing of their PV modules.

V.2. Uniform illuminated conditions

Figure (13) shows the P-V characteristics of PV modules at various solar irradiances.

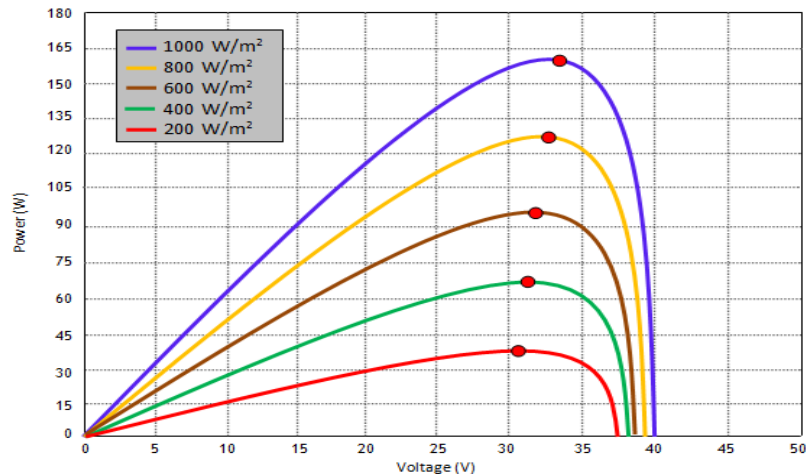


Figure 13. P-V characteristics of PV module

The characteristics describe the output power of the PV module within the functional operating voltage. The amount of the illuminated solar irradiance affects the output current generation. As the solar irradiance increased, PV cells in the module are able to release more electrons thus generating larger current. Hence, the output power is increased as the growing of solar irradiance.

The P-V characteristic illustrates non-linearity behavior with appearance of one MPP. At $1000W/m^2$ solar irradiance, the MPP is located at 34.4V with the power generation of 160W while at $200W/m^2$ solar irradiance, the MPP is relocated to 30.9V with the power generation of 33W.

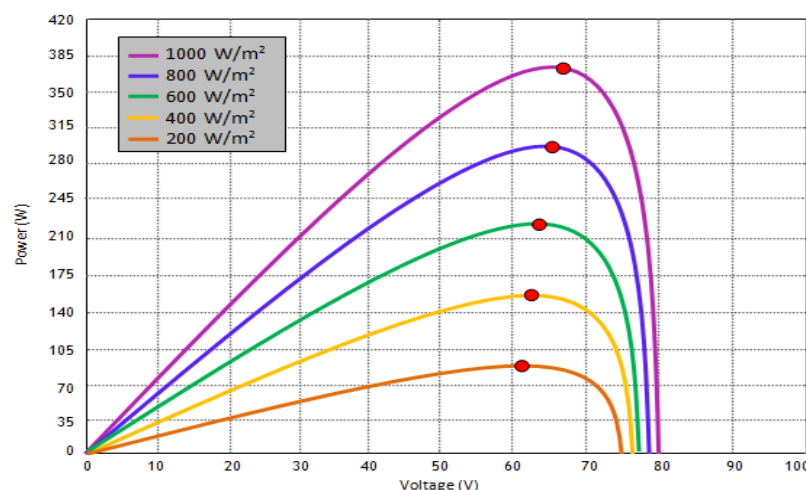


Figure 14. P-V characteristics of PV array

Figure (14) shows the P-V characteristics of the PV array. In this study, PV array is formed by two identical PV module connected in series. Therefore, PV array has two times larger operating voltage compared to the single PV module where in figure (14), the functional operating voltage range of PV array has two times of the voltage magnitude of PV module in figure (13). However, the series connected PV modules will not amplify the current generation. The current generated by the PV array is the same as PV module. Nevertheless, the array power generation will be two times greater than the output power produced by single PV module.

V.3. Partially shaded conditions

PV array under uniform illuminated conditions has nonlinear characteristic with the occurrence of one MPP in the P-V curve. However, when the PV array is under partially shaded conditions, the P-V characteristic becomes more complex. Multiple MPPs occur in the P-V characteristic due to the mismatched current generation by the PV array.

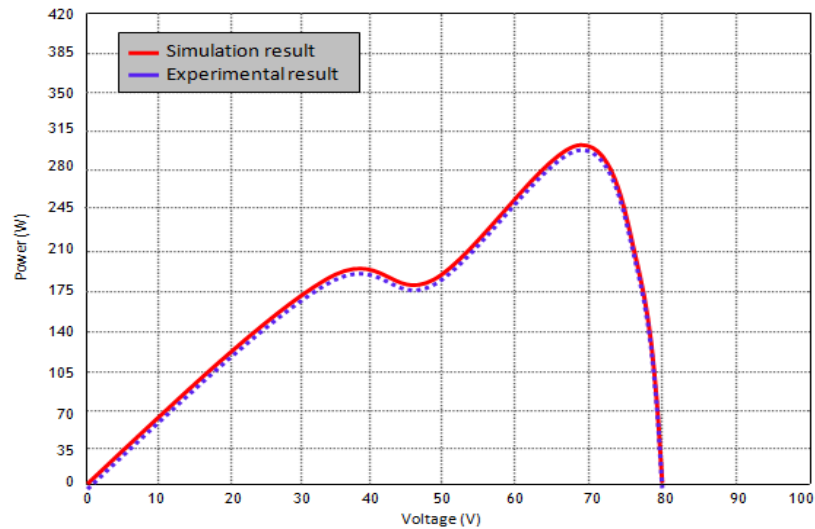


Figure 15. Characteristics of PV array where one of PV module shaded 20%.

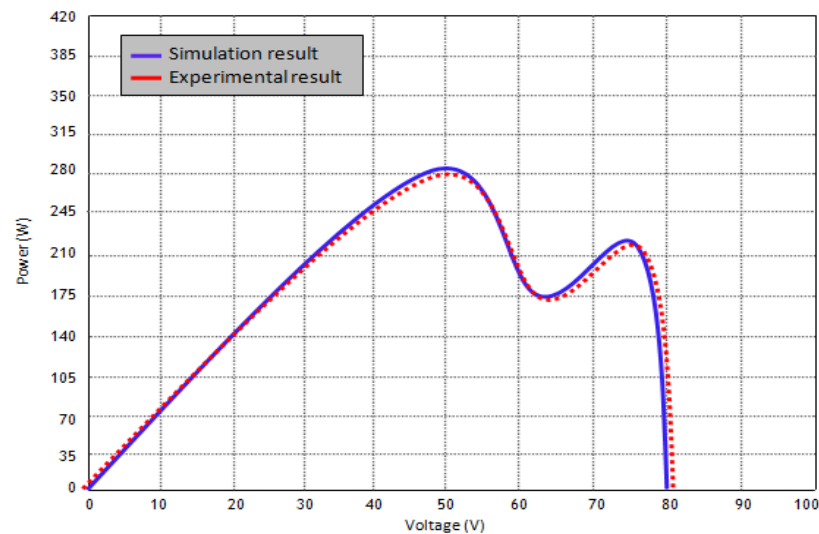


Figure 14. Characteristics of PV array where one of PV module shaded 5%.

Figure (15) and figure (16) illustrate the characteristics of PV array when one of the PV modules in the PV array is under shaded condition of 20% and 50% respectively. There are two MPPs in the P-V characteristic as shown in figure (15). It can be observed that PV array which is exposed to 20% partial shading has a local MPP of 39V and an absolute MPP of 68V. At local MPP, PV array will have approximately 208W power generation. However, if the PV array is operated at the absolute MPP, the power generation can be boost up to approximately 288W, 27.7% more than the local MPP.

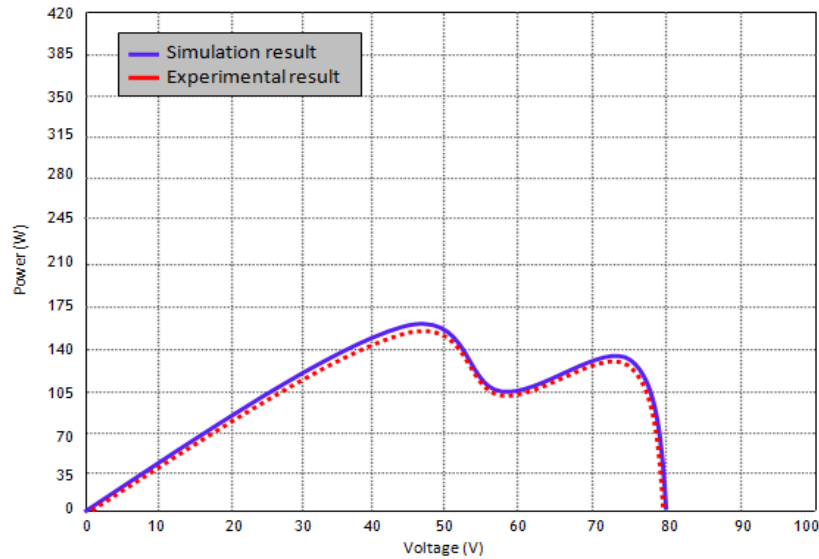


Figure 17. Characteristics of PV array where two of PV module shaded 20%.

Considering figure (17), where PV array is exposed to 50% partially shaded condition, the array presents a local MPP at operating voltage of 76V and an absolute MPP at 45.5V. PV array can generate output power of 138W in the local MPP operating condition. However, the efficiency of PV array will be enhanced if the PV array shifted the operation to the absolute MPP, where PV array can generate 38.67% larger power than the local MPP.

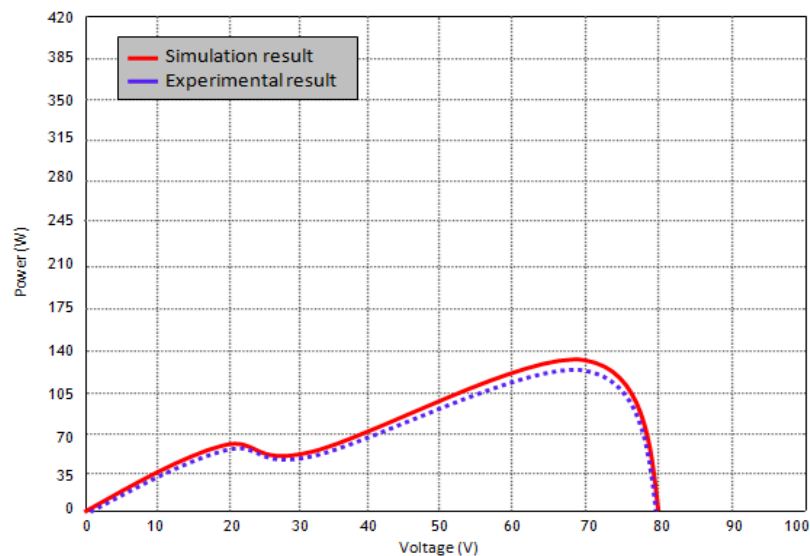


Figure 18. Characteristics of PV array where two of PV module shaded 50%.

When the PV array is exposed to various partial shading, multiple local MPPs might be occurred in the P-V characteristic. Figure (19) shows the PV characteristics when each PV modules in PV array is under 35% and 45% shaded conditions, whereas figure (20) shows the PV characteristics when each PV modules in the array is under 35% and 65% shaded conditions.

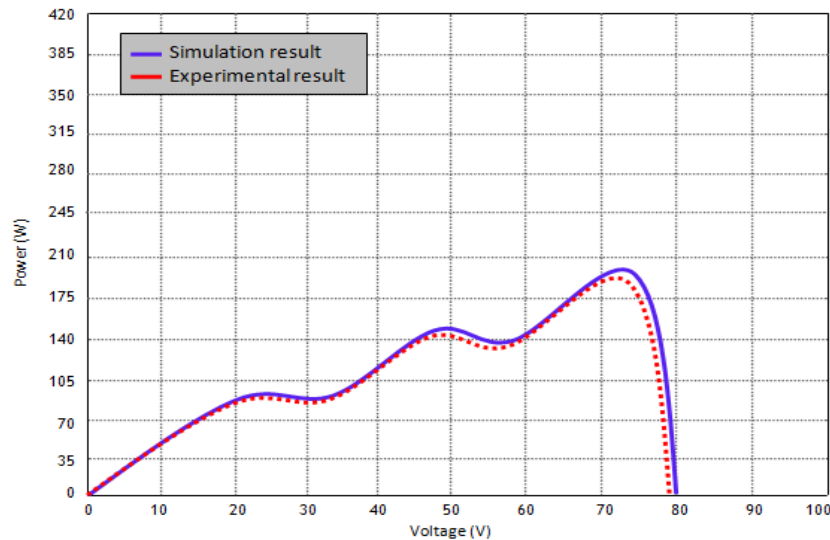


Figure 19. Characteristics of PV array where PV modules shaded 35% and 45%.

It can be noticed from figure (19), there are two local MPPs and one absolute MPP. The absolute MPP is located at the operating voltage of 76V. At local MPP of 22.5V, PV array generates output power of approximately 100W.

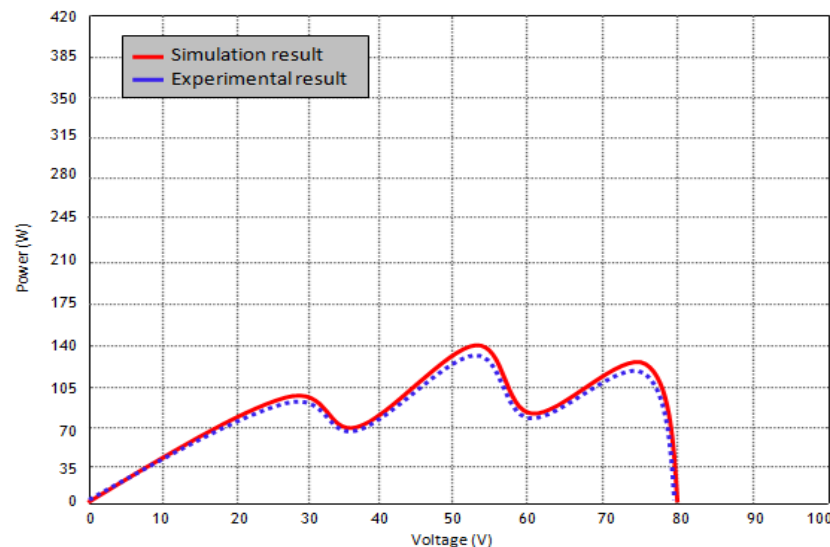


Figure 20. Characteristics of PV array where PV modules shaded 35% and 65%.

There is another local MPP beyond the local MPP of 22.5V, which is situated at the operating voltage of 48.5V. The PV array generates greater output power, 150W if it is operated at local MPP of 48.5V. However, at absolute MPP operating condition, the PV array produce the highest output power generation, which is 200W.

There are three MPPs being detected in figure (20). The MPPs are situated at the operating voltage of 29V, 54V and 76V respectively.

VI. Conclusion

In this paper, a new algorithm is introduced for an MPPT controller developed by means of the bond graph approach. The use of an MPPT control plays the important role of significantly increasing the efficiency of a photovoltaic generating system. Also this paper has demonstrated that the tracking speed of the proposed method is significantly improved compared to the other method.

References

- [1] Donny R., Dimas A. A., Takashi H., and S.; Partial Shading Detection and MPPT Controller for TCT Photovoltaic using ANFIS, *Int. J. on Elec. and Power Eng.*, Vol. 03, No. 02, May 2012
- [2] S. Silvestre, A. Boronat, A. Chouder; Study of bypass diodes configuration on PV modules, *Applied Energy* 86 (2009) 1632–1640
- [3] M. C. Glass, Improved solar array power point model with SPICE realization, in: *Proc. 31st Intersoc. Energy Convers. Eng. Conference IECEC*, vol. 1, 1996, pp. 286–291.
- [4] Y. T. Tan, D. S. Kirschen, N. Jenkins, A model of PV generation suitable for stability analysis, *IEEE Trans. Energy Convers.* 19 (4) (2004) 748–755.
- [5] A. Kajihara, A. T. Harakawa, Model of photovoltaic cell circuits under partial shading, in: *Proc. IEEE Int. Conf. Ind. Technol. ICIT*, 2005, pp. 866–870.
- [6] N. D. Benavides, P. L. Chapman, Modeling the effect of voltage ripple on the power output of photovoltaic modules, *IEEE Trans. Ind. Electron.* 55 (7) (2008) 2638–2643.
- [7] H. Patel, V. Agarwal, MATLAB-based modeling to study the effects of partial shading on PV array characteristics, *IEEE Trans. Energy Convers.* 23(1) (2008) 302–310.
- [8] H. Kawamura, K. Naka, N. Yonekura, S. Yamanaka, H. Kawamura, H. Ohno, K. Naito, Simulation of I–V characteristics of a PV module with shaded PV cells, *Solar Energy Mater. Solar Cells* 75 (3/4) (2003) 613–621.
- [9] M. C. Alonso-García, J. M. Ruíz, W. Hermann. Computer simulation of shading effects in photovoltaic arrays. *Renewable Energy* 31 (2006) 1986 – 1993.
- [10] M. C. Alonso-García, J. M. Ruíz. Analysis and modelling the reverse characteristic of photovoltaic cells. *Solar Energy Materials & Solar Cells* 90 (2006) 1105-1120.
- [11] A. Woyte, J. Nijs, R. Belmans. Partial shadowing of photovoltaic arrays with different system configurations: literature review and field test results. *Solar Energy* 74 (2003) 217-233.
- [12] N. Kaushika and N. Gautam, Energy yield simulations of interconnected solar PV arrays, *IEEE trans. energy conversion* 18, 2003 pp.127-134
- [13] H. Kawamura et al., Simulations of I-V characteristics of a PV module with shaded PV cells, *Solar energy materials & solar cells* 75, 2003 pp. 613-621
- [14] R. Bruendlinger et al., Maximum power point tracking performance under partially shaded PV array conditions, *21st European PV energy conference* 4-8 Sept. 2006
- [15] M. Garcia et al., Partial shadowing, MPPT performance and inverter configurations: observations at tracking PV plants, *Prog. Photovolt: Res. Appl.* 16, 2008, pp. 529-536
- [16] N. Chaintreuil et al., Effects of shadow on a grid connected PV system, *23rd European PV energy conference*, 2008, p.3417
- [17] Karnopp, D. C., and Rosenberg, R. C., (1975), *System dynamics a unified approach*, Wiley Interscience Publications, USA.
- [18] Mukherjee, A., and Karmakar, R. (2000), *Modelling and simulation of engineering systems through bond graphs*, Narosa Publishing House, India.

How to cite this paper:

Badoud A. MPPT Controller for PV Array under Partially Shaded Condition. Algerian Journal of Renewable Energy and Sustainable Development, 2019, 1(1),99-111.

<https://doi.org/10.46657/ajresd.2019.1.1.10>